ZERO SPIN ANGULAR MOMENTUM CONTROL: DEFINITION AND APPLICABILITY

MARKO POPOVIC
Biomechatronics Group, MIT Media Laboratory
20 Ames Street, Room 418, Cambridge, MA 02139, USA
Computer Science and Artificial Intelligence Laboratory, MIT
The Stata Center, 32 Vassar St., room 472, Cambridge, MA 02139,USA
marko@media.mit.edu

ANDREAS HOFMANN
Biomechatronics Group, MIT Media Laboratory
20 Ames Street, Room 054, Cambridge, MA 02139, USA
Computer Science and Artificial Intelligence Laboratory, MIT
The Stata Center, 32 Vassar St. room 275, Cambridge, MA 02139,USA
hofma@csail.mit.edu

HUGH HERR
Biomechatronics Group MIT Media Laboratory
20 Ames Street, Room 419, Cambridge, MA 02139, USA
hherr@media.mit.edu

In this paper, we seek control strategies for legged robots that produce resulting kinetics and kinematics that are both stable and biologically realistic. Recent biomechanical investigations have found that spin angular momentum is highly regulated in human standing, walking and running. Motivated by these biomechanical findings, we argue that biomimetic control schemes should explicitly control spin angular momentum, minimizing spin and CM torque contributions not only local in time but throughout movement tasks. Assuming a constant and zero spin angular momentum, we define the Zero Spin Center of Pressure (ZSCP) point. For human standing control, we show experimentally and by way of numerical simulation that as the ZSCP point moves across the edge of the foot support polygon, spin angular momentum control changes from regulation to non-regulation. However, even when the ZSCP moves beyond the foot support polygon, stability can be achieved through the generation of restoring CM forces that reestablish the CM position over the foot support polygon. These results are interesting because they suggest that different control strategies are utilized depending on the location of the ZSCP point relative to the foot support polygon.

Keywords: biomechanics, biped, balance, angular momentum, human.

1. Introduction

The control of balance and postural stability in legged systems has been studied extensively by both roboticists and biomechanicists. Recently, the control of whole body rotational dynamics through the explicit control of angular momentum has been discussed in the literature.[1-10] In this paper, we further discuss the high level control objective of spin angular momentum regulation and the Zero Spin Model discussed previously.[1-5] We contrast our model to the recently proposed "rate of change of angular momentum model" that suggest that the minimization of CM torque should serve as a simple measure for capturing system stability.[6] We argue that torque information is insufficient for addressing postural stability. Based on our biomechanical findings we anticipate that minimization of both spin angular momentum and torque is more appropriate for stable and biomimetic controllers. Using biomechanical and numerical simulation studies of human standing movements, we test different control regions based on the degree of spin angular momentum regulation.

2. Zero Spin Control and the ZSCP Point

Biomechanical investigations have determined that a large class of human movements,[1-5] including standing, walking and running, support conservation of spin angular momentum, i.e. total angular momentum about the body's center-of-mass (CM), $\vec{S} = \vec{L}(\vec{r}_{CM})$, or

$$\vec{L}(\vec{r}_{CM}) = \mathbf{0} . \tag{1}$$

Spin angular momentum is a conserved physical quantity for isolated systems where no external moments act on a body's CM. However, in the case of legged locomotion, where the body interacts with the environment (ground reaction forces), there is no ***a priori*** reason for this relationship to hold. It is asserted here that spin angular momentum is highly regulated ($\vec{S} \approx 0$) by the central nervous system *throughout a movement cycle*.

Since spin angular momentum is highly regulated for many human movement tasks the net spin torque, i.e. moment about the CM point, $\vec{\tau}(\vec{r}_{CM})$ is negligible, suggesting a coupling between the resulting ground reaction force, $\vec{F}$, the location of the CM, $\vec{r}_{CM}$, and center of the pressure (CP), $\vec{r}_{CP}$, also known as Zero Moment Point (ZMP),[11] or

$$\vec{F} = k \; \delta \vec{r} \;, \tag{2}$$

where $\delta \vec{r} = \vec{r}_{CP} - \vec{r}_{CM}$ and $k = F_Z / \delta z = -F_Z / z_{CM}$. Eq (2) is consequence of $\vec{\tau}(\vec{r}_{CM}) = 0$.

Critical to advancing humanoid control systems that reproduce human like movements, a humanoid control system must minimize the spin angular momentum. On these lines the Zero Spin Control strategy representing any control framework that tries to minimize global spin angular momentum has been proposed.[1] If the whole body state is such that spin is not zero then the zero spin controller will apply corrective torques to minimize the spin quantity. A necessary but not sufficient condition for the minimization of global spin angular momentum throughout a movement cycle is that the physical CP tracks the Zero Spin Center of Pressure (ZSCP), which may be defined using Eq. (2), or

$$\vec{r}_{ZSCP} = \vec{r}_{CM} + \frac{\vec{F}}{k} . \tag{3}$$

Clearly, as shown in Fig. 1, the ZSCP and CP points do not coincide if horizontal component of spin torque is different from zero, i.e. $\vec{\tau}(\vec{r}_{CM})_{horizontal} \neq 0$.
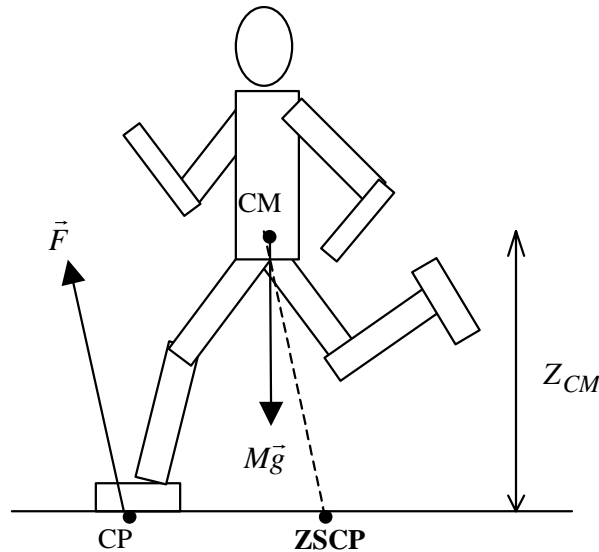

Fig. 1. The Zero Spin Center of Pressure (ZSCP) point.

Using space-time optimization techniques[12] and a morphologically realistic human model, Popovic et al. predicted biologically realistic joint angle trajectories when 1) global spin angular momentum was minimized, 2) the physical CP tracked the ZSCP trajectory and in addition 3) the sum of joint torque-squared were minimized.[4]

Goswami and Kallem recently proposed a similar, but distinct, control strategy where CM torque is minimized instead of spin angular momentum.[6] It is well known that the rate of change of angular momentum is equal to the net torque about the CM. Therefore this control strategy also tries to keep spin angular momentum constant but without preference for the actual value of that constant. However, the human body is not a wheel that can rotate at constant non-zero angular momentum. Therefore, if rotational stability is in advance restricted to one constant value of the angular momentum in horizontal plane than this value oaths to be zero. Obviously a constant and non-zero value of spin angular momentum would eventually lead to instabilities in postural balance. Hence, we state here that for legged systems, it is not sufficient for the controller to only minimize CM torque, but rather the system must also minimize the global spin angular momentum.[1-5]

3. Zero-Spin Control: Region of Applicability

Stability in bipedal systems does not always require that spin angular momentum remains small. Clearly, there exist many bipedal movements for which large variations in spin angular momentum occur without loss of system stability. Examples of unsteady movements when spin angular momentum is non-zero are locomotory turning maneuvers and double support swiveling actions. In this section we present biomechanical evidence in support of the idea that bipedal stability does not always require spin angular momentum minimization by a control system. In addition, our experimental data supports the hypothesis that two distinct postural balance strategies are active during human balance. In a first strategy, the physical CP tracks closely the ZSCP point, keeping the CM moments small and the spin angular momentum near zero. In a second strategy, the ZSCP falls outside the foot support polygon, forcing the body to counteract destabilizing CM moments through a re-distribution of body segment orientations. Finally, we discuss a simple thought experiment related to the dynamics of balance beam balancing and show that there are situations when system instability may arise even when spin angular momentum is regulated.

3.1. *Biomechanical Investigation: Hula-Hoop Twirling Movements*

As explained in the previous section, the actual *CP*, in biological or robotic systems, will differ from the *ZSCP* if spin angular momentum is not precisely regulated. In this context non-regulation means that spin torque is different from zero. As discussed in Popovic et al. significant separation distances between the *ZSCP* and the actual *CP* are expected for at least two distinct physical situations:[4]

(i)   When the ground reaction force is so large that the *ZT*CP point moves outside the foot-support polygon.

(ii)   When sudden and large turning motions occur (non-zero vertical torque) rotating the *ZTCP* point away from the actual *CP* location.

In the first case, the switching of control strategy from regulation to non-regulation was recently observed for hula-hoop twirling movements. For these rotational movements, ground reaction forces, *CP* trajectory, and kinematic data were obtained in the Gait Laboratory of Spaulding Rehabilitation Hospital, Harvard Medical School. For the standing task of interest, a healthy normal subject rotated his hips (similar to how one twirls a hula hoop) at an increasing and then decreasing speed for about ten seconds. The ground reaction forces were measured using two AMTI forceplates (model OR6-5-1,
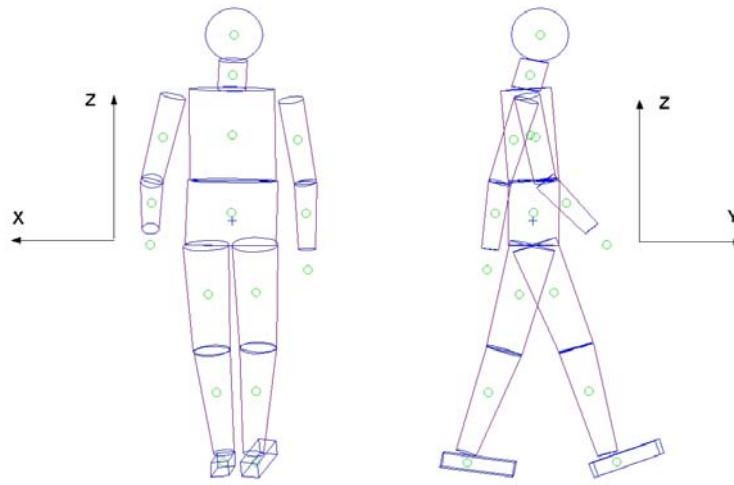
Fig. 2. Morphologically realistic human model.

AMTI, Newton, MA) at the frequency of 1080 Hz. The forceplates had a precision of approximately 0.1 Newton. The limb trajectories were acquired using an infrared VICON Motion Capture system (VICON 512, Oxford Metrics, Oxford, England). Thirty-three markers were placed on the subject's body: sixteen lower body markers, five trunk markers, eight upper limb markers and four head markers. Motion data were gathered at a frequency of 120 Hz. Depending on the position and movements of the subject, the VMC could detect marker positions with a precision of a few millimeters.

The human model,[4] used for analysis consisted of 16 links: right and left feet, shanks, thighs, hands, forearms, upper arms, the pelvis-abdomen region, the thorax, the neck and the head. The feet and hands were modeled as rectangular boxes. The shanks, thighs, forearms and upper arms were modeled as truncated cones. The pelvis-abdomen link and the thoracic link were modeled as elliptical slabs. The neck was modeled as a cylinder and the head was modeled as a sphere. This model is shown in Fig. 2. About twenty physical measurements of the subject's links dimensions were taken to accurately model the subject. Based on the links' dimensions the link's masses and densities were modeled to closely match the experimental values.[13-14] The human model had a total of 38 degrees of freedom; 32 internal degrees of freedom (12 for the legs, 14 for the arms and 6 for the rest) and 6 external degrees of freedom.

When the rotational movements first began, while joint speeds were still small, the *ZSCP* was found to be inside the foot support polygon. However, when overall speed became substantial, the *ZSCP* left the foot support polygon. It was observed that while the *ZSCP* was confined within the foot-support polygon, the actual *CP* was found to track the *ZSCP* with reasonable precision. However, immediately after the *ZSCP* left the foot-support polygon, the actual *CP* returned to the proximity of the center of the foot-support polygon as the *ZSCP* continued to operate outside the foot support polygon.
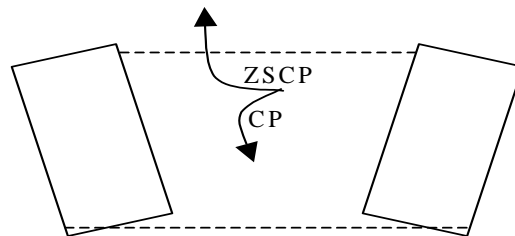

Fig. 3. When ZSCP left the foot support polygon, CP returned to the center of the foot support polygon.

The observation that the *CP* tracked *ZSCP*, while inside the foot support polygon, was expected. As stated earlier, the same phenomenon was observed for normal human walking and motivated the biomimetic zero spin control strategy.[1-5] By definition, the *CP* cannot leave the foot support polygon and hence, the CP cannot possibly track the *ZSCP* after the *ZSCP* has left the foot support polygon. The instant when the *ZSCP* point left the foot support polygon, therefore, indicated the instant when non-zero spin torques were *necessarily* present in the system. However, it was not anticipated that the *CP* would return to the center of the foot support polygon after the *ZSCP* left the foot support polygon. If the control strategy only tries to minimize the spin and the torque as suggested with Zero Spin Control,[4] one would expect the *CP* trajectory to be very close to the edge of the foot support polygon – but that was not supported by our experimental findings.

We dub this interesting phenomenon, this "switching mechanism" coinciding with the moment when *ZSCP* crosses the edge of the foot support polygon, as a "phase transition" in between two distinct postural balance strategies suggesting a change in collective integrated behavior of all joints.
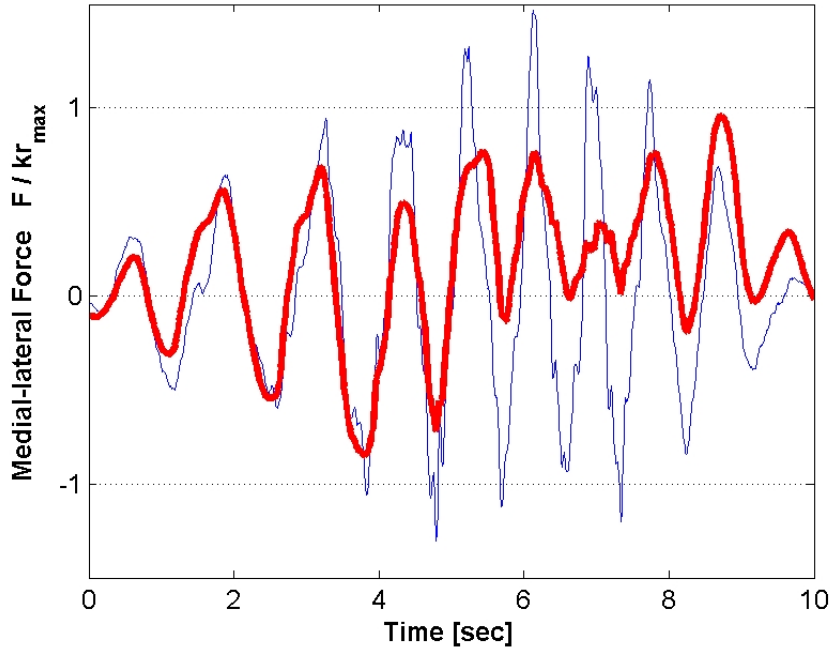

Fig. 4. The experimental data (thin line) and zero-spin model (thick line) dimensionless ground reaction forces for the hula-hoop twirling like motion. Plotted vertically is a dimensionless force equal to the medial-lateral ground reaction force divided by the global body stiffness (defined in Eq. (2)) and the maximum radius of the foot support polygon. Significant *CM* torques occurred when the dimensionless horizontal force were greater than one.

We showed previously that zero torque condition is equivalent to the non-linear coupling between *CP, CM* and ground reaction force.[1-5] This coupling may be tested by comparison of zero spin model force with experimental force data. In Fig. 4, we show model and experimental forces for hula-hoop twirling body motions. Note that a large difference between the two curves means a large spin torque present in the system. Immediately after the *ZSCP* left the foot support polygon at $t \approx 4$ s, the agreement between model and measured force became significantly poorer.
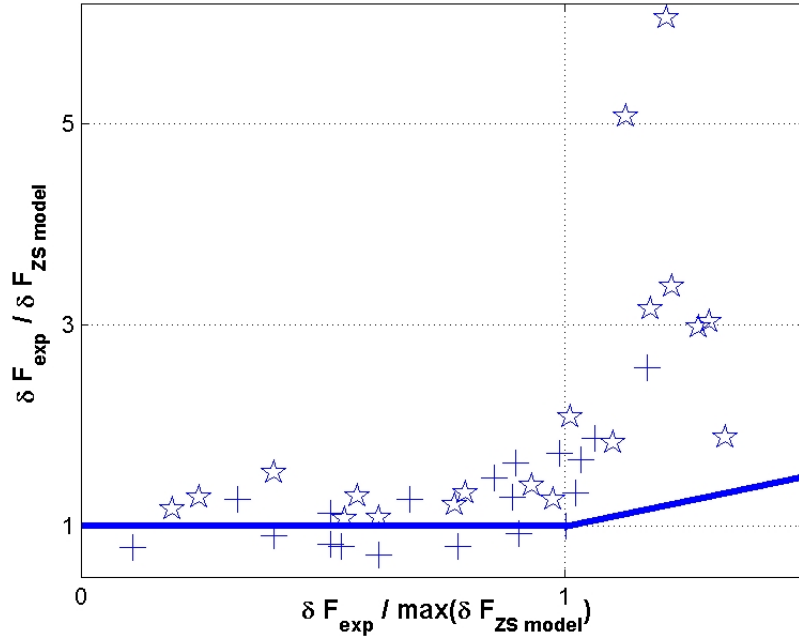
Fig. 5. The balance "phase transition" illustrated with crosses and stars for anterior-posterior and medial-lateral directions, respectively. Solid line corresponds to the theoretical prediction based purely on the zero spin control strategy.

For each half-period of hula-hoop cyclic motion, we found the peak force difference (i.e. max-min) for both experimental and model forces, i.e. $\delta F_{\exp}$ and $\delta F_{ZS\,model}$, respectively. In Fig. 5, we use these quantities to further illustrate the "phase transition" behavior between two control strategies. Dimensionless $\delta F_{\exp}/\delta F_{ZS\,model}$ versus $\delta F_{\exp}/\max(\delta F_{ZS\,model})$ is shown for both anterior-posterior and medial-lateral directions. Here $\max(\delta \vec{F}_{ZS\,model})$ is defined as $\dfrac{|F_z|}{Z_{CM}}\max(\vec{r})$ with $\max(\vec{r})$ equal to the maximum radius of the foot support polygon (i.e. with direction defined by the actual $(\vec{r}_{CM}-\vec{r}_{CP})_{horizontal}$ direction). If the control strategy is designed to minimize the spin as suggested in [1-5] all the points should be grouped about the solid line. While this is closely satisfied for $\delta F_{\exp}/\max(\delta F_{ZS\,model}) \leq 1$ it is clearly not true for

$\delta F_{\exp}/\max(\delta F_{ZS\,model}) > 1$ when $ZSCP$ point is outside the foot support polygon.

One possible rationale for this observation is that with large force and torques the error in CP is likely to be large. Therefore in the interplay between several control targets one might prefer to minimize the possibility of CP being at the edge of the foot support polygon or alternatively in the single support phase the Foot Rotation Indicator (*FRI*)[15] point being beyond this enclosed area. Clearly the best way to do so is to position the *CP* in the center of foot support polygon.

In the next subsection we present a thought experiment clearly illustrating that there are situations when system instability may arise even when spin angular momentum is regulated.

3.2. *Thought Experiment: Balance Beam Balancing*

Consider the problem of postural balance in the coronal plane for the situation when a gymnast is attempting to remain upright on a balance beam. As a simplification, imagine that the beam has infinitesimal thickness and that the *CP* trajectory is confined to a single point. We set the *CP* to be located at origin of the reference frame, or $x_{CP} = 0$. Clearly, the body posture is statically unstable and the control goal for static equilibrium is to have the *CM* positioned just above the *CP* location, or $x_{CM} = 0$.

Now consider a small perturbation such that $x_{CM} > 0$, $v_{CM} = 0$, $L^y(\vec{r}_{CM}) = 0$ (i.e. zero spin) and $\tau^y(\vec{r}_{CM}) = 0$ (i.e. zero spin torque implying *ZSCP=CP*). If the Zero Spin control strategy is to be satisfied then torque should remain zero. However, this situation requires that the ground (beam) reaction force vector is parallel to $\vec{r}_{CM} - \vec{r}_{CP}$. Therefore, the horizontal force is positive, further destabilizing the gymnast's posture.
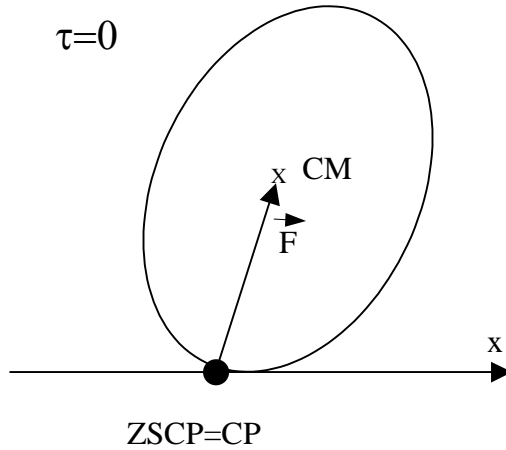

Fig. 6. The Zero Spin Control strategy acting alone would further destabilize an unstable posture.

Clearly, in this situation the right way to balance is to have a negative restoring force that will counteract the destabilizing gravitational force to bring the *CM* point just above the *CP* point. However, this action requires that the *ZSCP* point moves in the positive *x* direction, to the right of the CM point, and away from the *CP* point and the foot support polygon. Of course when the gymnast's posture is finally stabilized, the *ZSCP* point will coincide with the *CP* point; however, in terms of the postural control, it is the intermediate *ZSCP* trajectory that matters.
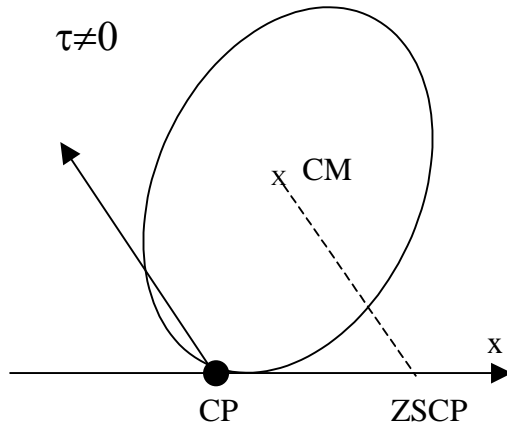
Fig. 7. The ZSCP point should move to the right of the CM point in order to stabilize the unstable posture.

Control issues are much subtler when the *CP* point is confined to a very small area. From a knowledge of system state, the *CM* location can be computed. With both the *CP* and *CM* positions defined, there is then a unique one-to-one relationship between the global dynamical variables, or the CM torque and the total ground reaction force. If during particular physical situation, the control of the translational *CM* degree of freedom is more important for stability than the control of the global rotational degree of freedom, then the CM torque may be nonzero and spin non-regulated (in terms of emergent behavior).

In the next section we introduce the simple toy model and numerically estimate its regions of spin regulation, non-regulation and instability.

4. Balancing Toy Model

We now describe a simple model that illustrates the previously discussed concepts. The model's simplicity allows for use of a relatively simple, direct control law, and allows for comprehensive analysis of stability in the presence of significant disturbances. Although the model has many simplifying assumptions, it still illustrates key aspects of balance behavior. For example, this model shows clearly when and why the *ZSCP* has to leave the foot support polygon.

The controller described here is related, conceptually, to the much more complex controller described previously.[16] The latter is a controller for a much more complex plant, and it uses a feedback linearization approach, combined with a quadratic programming algorithm to solve an optimal multivariable control problem. Although this approach is elegant in its formulation, it is computationally intensive, and it is difficult to make assertions about stability because the control actions are taken as a result of the complex optimization algorithm machinery, rather than by more conventional, direct control laws. Thus, the reason for investigating the simplified model presented here is to see whether simpler, more direct control laws could be used, and to compute stability bounds.

4.1 *Model Definitions*

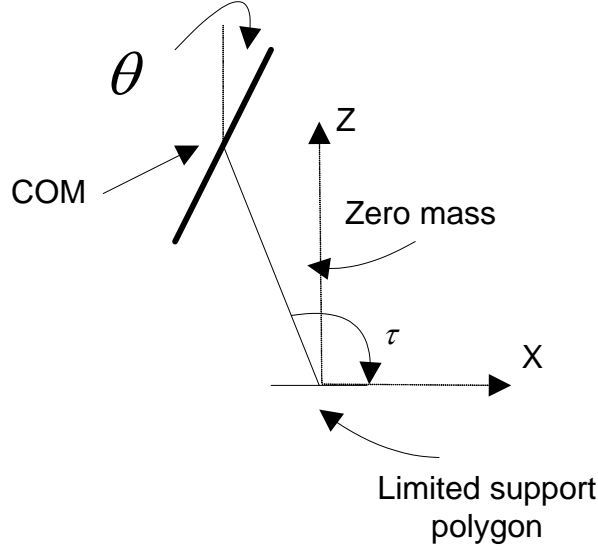Consider the simplified two-link 2-D model shown in Fig. 8.

Fig. 8. The Simplified Toy Model..

The model consists of three links: a body link representing the upper body, head, arms and swing leg, lumped together, a stance link representing the stance leg, which is assumed to have zero mass, and a foot link (base of support), which is aligned with the ground and which has limited extent. The joint between the foot link and the stance leg is the "ankle" joint, and the joint between the stance leg and the body is the "hip" joint. Both of these joints are actuated. The body link is symmetric about the hip joint, so the *CM* of the system is always located at this joint.

The torque balance equation for this model is

$$\tau(0) = \tau_{ankle} = \tau_{orbital} + \tau(x_{CM}) \tag{4}$$

where, τ_{ankle} is the "stance ankle" torque in Fig. 8, given by

$$\tau_{ankle} = x_{FRI}\, M_1\left(\ddot{z}_{CM} + g\right) \tag{5}$$

and x_{FRI} is the location of the FRI point.[15] $\tau_{orbital}$ is the torque of the COM about the stance ankle joint (origin), and is given by

$$\tau_{orbital} = M_1 x_{CM}\left(\ddot{z}_{CM} + g\right) - M_1 \ddot{x}_{CM}\, z_{CM} \tag{6}$$

where M_1 is the mass of the body link . This is also the rate of change of orbital angular momentum of the system. $\tau(x_{CM})$ is the torque about the *CM*, i.e. spin torque, given by

$$\tau(x_{CM}) = -I\ddot{\theta} \tag{7}$$

where I is the inertia of the body link. This is the rate of change of the spin angular momentum about the *CM*.

Eq. (4) is equivalent to defining *FRI* equation,[15] and Eq. (5 – 7) represent a specialization of this equation for the simplified model. Eq. (4) clearly shows the tradeoff between orbital and spin terms. Note that if there is no actuation at the stance ankle, then orbital and spin components must balance, as would be expected from conservation of angular momentum.

Now, suppose that the support polygon extends from the origin in both directions along the x axis by an amount $x_{\text{supp\_bound}}$. To prevent the foot from rolling, the stance ankle torque must stay within the following limit:

$$|\tau(0)| \le |x_{\text{supp\_bound}}| M_1 (\ddot{z}_{CM} + g) = \tau_{\max} \qquad (8)$$

Note that this corresponds to the *FRI* point staying within the support polygon,[15]

$$|x_{FRI}| \le |x_{\text{supp\_bound}}| \qquad (9)$$

4.2. *Balance Control*

Let's suppose that the primary (most important) control output is x_{CM}. Suppose that $\ddot{x}_{CM}$ is computed based on a simple PD control law. Then, assuming appropriate feedback linearization of the system, the trajectory for x_{CM} is known analytically for all time given any initial condition (it is the solution of a simple linear second-order system). Since z_{CM} is directly related to x_{CM} via simple trigonometric functions, $\tau_{orbital}$ can be computed using Eq. (6), so its trajectory is also known.

Specifically, assuming a simple PD control law with position gain k_p and damping gain k_d, the general solution for x_{CM} for given set point, x_{set}, is

$$x_{CM} = e^{\alpha t}(K_1 \cos(\beta t) + iK_2 \sin(\beta t)) + x_{set} \qquad (10)$$

$$\dot{x}_{CM} = e^{\alpha t}(\beta(-K_1 \sin(\beta t) + iK_2 \cos(\beta t)) + \alpha(K_1 \cos(\beta t) + iK_2 \sin(\beta t)))$$

where

$$K_1 = x_{CM}(0) - x_{set} , \quad K_2 = i(\alpha K_1 - \dot{x}_{CM}(0))/\beta$$

$$\alpha = \frac{-k_d}{2} , \qquad \beta = \frac{-i\sqrt{k_d^2 - 4k_p}}{2} \qquad (11)$$

The acceleration trajectory is computed using Eqs. (10-11), along with the PD control law

$$\ddot{x}_{CM} = -k_d \dot{x}_{CM} - k_p x_{CM} \qquad (12)$$

Vertical center of mass position is computed using

$$z_{CM} = \sqrt{l^2 - x_{CM}^2} \qquad (13)$$

Taking the second derivative yields $\ddot{z}_{CM}$. Values for x_{CM}, $\ddot{x}_{CM}$, z_{CM}, and $\ddot{z}_{CM}$ can be substituted into Eq. (6) to compute $\tau_{orbital}$.

Following the approach of using slack variables in the previous optimal controller implementation,[16] it is useful to separate $\tau(x_{CM})$ into two parts:

$$\tau(x_{CM}) = \tau_{spin\_des} + \tau_{spin\_slack} \qquad (14)$$

where τ_{spin_des} is computed by a PD control law. Eq. (4) then can be written as

$$\tau_{orbital} + \tau_{spin\_des} = \tau(0) - \tau_{spin\_slack} \qquad (15)$$

The left-hand side can be computed analytically for any initial condition in the manner described in the previous section. The values on the right-hand side need to be determined, subject to the restriction on maximum ankle torque, and Eq. (15). The following control law makes $|\tau_{spin\_slack}|$ as small as possible.

If

$$\left| \tau_{orbital} + \tau_{spin\_des} \right| \le \tau_{\max}$$

then

$$\tau(0) = \tau_{orbital} + \tau_{spin\_des}$$

$$\tau_{spin\_slack} = 0$$

else

$$\tau(0) = \tau_{\max}$$

$$\tau_{spin\_slack} = \tau(0) - \tau_{orbital} - \tau_{spin\_des}$$

Note that this control law behaves in a manner similar to the one in the optimal controller implementation.[16] The difference is that this one is direct; it does not require running a quadratic program optimizer.

All that remains in order to prove stability is to show that τ_{spin_slack} is transient and appropriately bounded. Actually, it is more precise to show that $\tau(x_{CM})$ and its integrals (and therefore $\ddot{\theta}$ and its integrals) are transient and appropriately bounded.

4.3. *Stability and Bounds on Spin Torque*

Because x_{CM} behaves linearly, as discussed previously, this output is stable, as is the directly related value $\tau_{orbital}$. As mentioned previously, the remaining task is to show that $\tau(x_{CM})$ and its integrals (and therefore $\ddot{\theta}$ and its integrals) are transient and appropriately bounded.

Assuming, for simplicity, that $I = 1$ Eq. (4) simplifies to $\tau(x_{CM}) = -\ddot{\theta}$. Thus, Eqs. (15, 13, 12, and 10) can be used to compute $\ddot{\theta}$. This is then integrated (either numerically, or analytically) to compute trajectories for θ, $\dot{\theta}$. The constants of integration are determined from initial conditions on $\theta, \dot{\theta}$. Thus, it is very easy to check whether bounds on $\theta, \dot{\theta}$ will be violated. In essence, the gap between the initial values for $\theta, \dot{\theta}$ and the bounds on $\theta, \dot{\theta}$ is a "reservoir" of spin torque $\tau(x_{CM})$ that can be used to assist $\tau(0)$. This reservoir is limited. Its size depends on the initial values for $\theta, \dot{\theta}$ and the bounds on $\theta, \dot{\theta}$.

Trajectories using the above described methods are shown in Fig. 9.
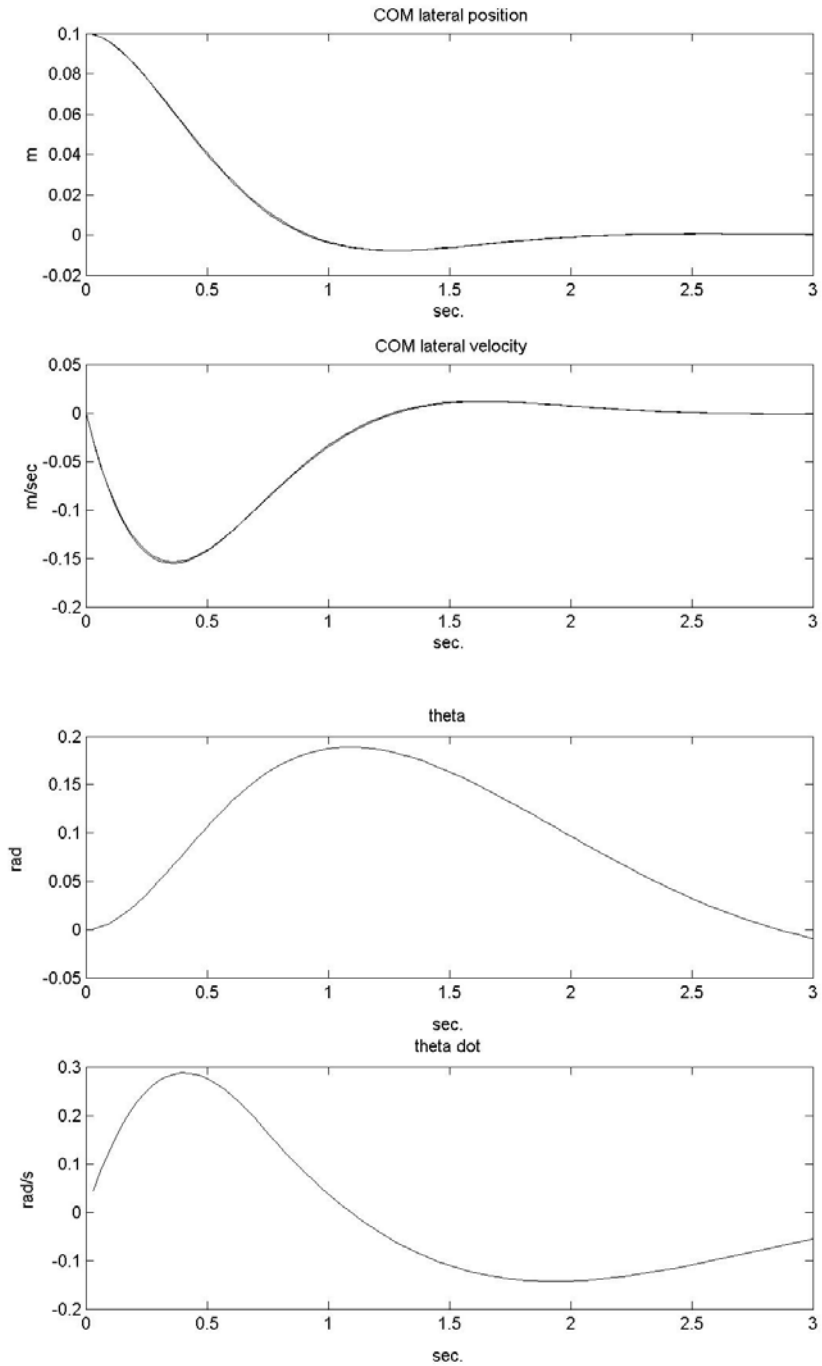
Fig. 9. CM lateral position, CM lateral velocity, theta, and angular velocity are plotted versus time. As can be seen, theta deviates significantly from its desired value of 0, but theta and the derivative of theta (theta dot) do stay within reasonable bounds (maximum rotation of the body link is 0.2 radians).
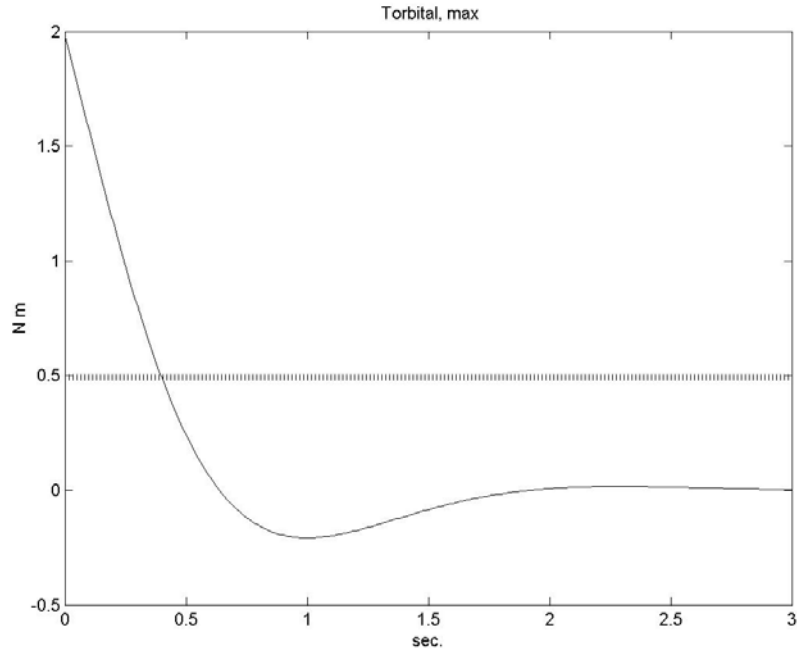
Fig. 10. Solid line shows orbital torque versus time. Dotted line shows maximum ankle torque.
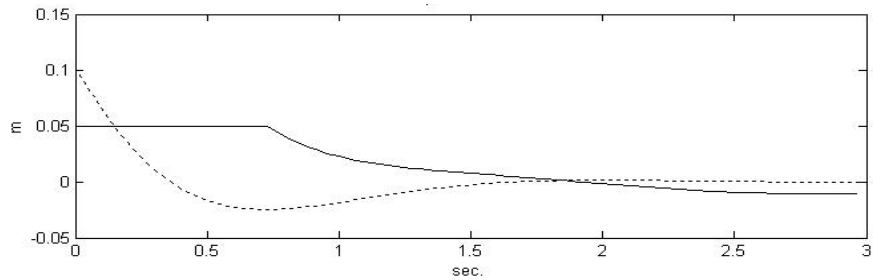

Fig. 11. Solid line shows the *CP* point, which stays within the support polygon boundary of 0.05 m. Dotted line shows the *ZSCP* point. Note that this begins outside the foot support polygon boundary. As can be seen, the *CP* remains within the bounds of the support polygon, but the *ZSCP* does not. This is consistent with the bulge in theta in the Fig. 9.

The methods described above can also be used within a simple optimization algorithm to determine maximum initial *CM* x position for a range of initial theta positions, as shown in the following plot.
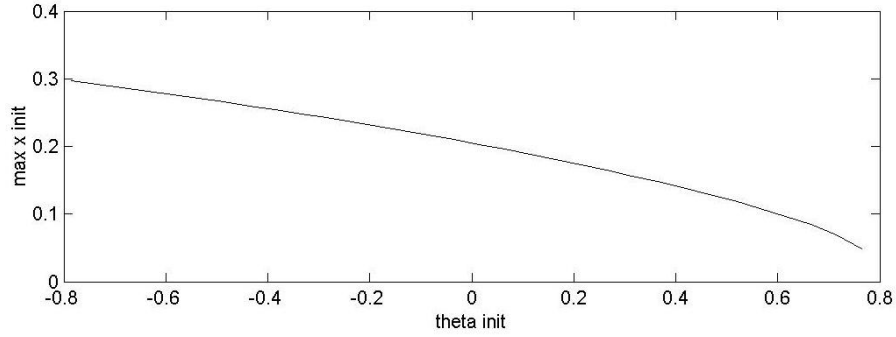
Fig. 12. Maximum stable initial lateral CM deflection as a function of initial hip joint angle position. As the hip joint angle increases, the reservoir of stability is reduced, and the maximum initial lateral *CM* deflection such that the system is stable decreases. Eventually, it reaches 0.05, which is the limit of the support polygon. Within the support polygon, the system can always be stabilized using ankle torque only, so initial hip joint angle is no longer a factor.

A similar technique can be used to determine maximum initial *CM* x position for a range of initial *CM* x velocities, as shown in the following plot.
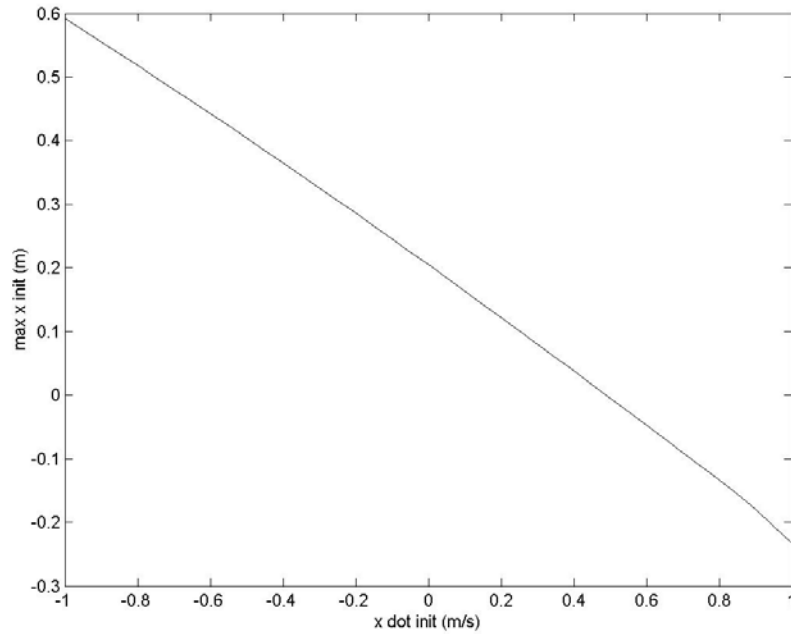

Fig. 13. Maximum stable initial lateral CM deflection as a function of initial lateral CM velocity. If the CM is already moving towards the origin (in the negative direction in this case), the initial deflection can be large. If the CM point is moving away from the origin (in the positive direction), the initial deflection has to be smaller if the system is to stabilize.

There is an important difference in the way that $\tau_{orbital}$ and τ_{spin_des} are pre-determined. Because $\tau_{orbital}$ is solely a function of the primary output, it is pre-determined completely and independently for all time. τ_{spin_des}, on the other hand, is a function of

$\tau(x_{CM})$, which is affected by τ_{spin_slack}, which, in turn, is affected by $\tau_{orbital}$. Thus, τ_{spin_des} can be pre-determined, but as a function of $\tau_{orbital}$; it is not independent.

5. Summary

In this paper, we seek control strategies for legged robots that produce resulting kinetics and kinematics that are both stable and biologically realistic. Since the regulation of spin angular momentum has been observed in human standing, walking and running movements,[1-5] we argue that biomimetic control schemes should explicitly control spin angular momentum, minimizing spin and *CM* torque contributions not only local in time but throughout movement tasks. Assuming a constant and zero spin angular momentum, we define the Zero Spin Center of Pressure (*ZSCP*) point. For human standing control, we show experimentally and by way of numerical simulation that as the *ZSCP* point moves across the edge of the foot support polygon, spin angular momentum control changes from regulation to non-regulation. However, even when the *ZSCP* moves beyond the foot support polygon, stability can be achieved through the generation of non-zero spin angular momentum and restoring *CM* forces that reestablish the CM position over the foot support polygon. In the design of control systems for legged biomimetic systems, we feel the location of the *ZSCP* point relative to the foot support polygon is an important design consideration.

Acknowledgment

References

1. M. Popovic, W. Gu, and H. Herr, "Conservation of Angular Momentum in Human Movement," in *MIT AI Laboratory-Research Abstracts, 2002*, (2002), pp. 231-232.

2. H. Herr, G. P. Whiteley, D. Childress, "Cyborg Technology--Biomimetic Orthotic and Prosthetic Technology," *Biologically Inspired Intelligent Robots*, Bar-Cohen, Y. and C. Breazeal, Eds., SPIE Press, Bellingham, Washington, 2003, pp. 103-143.

3. W. Gu, "The Regulation of Angular Momentum During Human Walking", Undergraduate Thesis, Physics Department, MIT, June 2003.

4. M. Popovic, A. Hofmann and H. Herr, "Angular Momentum Regulation during Human Walking: Biomechanics and Control," in *IEEE International Conference on Robotics and Automation (ICRA)*, 2004, pp. 2405-2411.

5. M. Popovic and H. Herr, "Angular Momentum Regulation during Human Walking," *Journal of Experimental Biology,* [in prep.], (2004).

6. A. Goswami and V. Kallem, "Rate of change of angular momentum and balance maintenance of biped robots," in *IEEE International Conference on Robotics and Automation (ICRA)*, 2004, pp. 3785-3790.

7. N. E. Sian, K. Yokoi, S. Kajita, F. Kanehiro and K. Tanie,"Whole-body teleoperation of a humanoid robot – a method of integrating operator's intention and robot's autonomy," in *IEEE International Conference on Robotics and Automation (ICRA)*, 2003, pp. 1613-1619.

8.   S. Kajita, F. Kanehiro, K. Kaneko, K. Fujiwara, K. Harada, K. Yokoi, H. Hirukawa, "Resolved Momentum Control: Humanoid Motion Planning based on the Linear and Angular Momentum," in *International Conference on Intelligent Robots and Systems (IROS)*, 2003, pp. 1644-1650.

9.   S. Kudoh, and T. Komura, "C2 Continuous Gait Pattern Generation for Biped Robots," in *International Conference on Intelligent Robots and Systems (IROS)*, 2003.

10.   S. Kajita, T. Nagasaki, K. Kaneko, K. Yokoi and K. Tanie,"A Hop towards Running Humanoid Biped," in *IEEE International Conference on Robotics and Automation (ICRA)*, 2004, pp. 629-635.

11.   M. Vukobratovic, A. A. Frank and D. Juricic, "On the stability of biped locomotion," *IEEE Trans. Bio-Medical Engineering*, Vol. BME-17, No. 1, 1970, pp. 25-36.

12.   Z. Popovic, A. Witkin, "Physically Based Motion Transformation", in *Siggraph* 1999.

13.   A. R. Tilley and H. Dreyfuss, "The measure of man and woman," *Whitney Library of Design*, an imprint of Watson-Guptill Publications, New York. (1993)

14.   D. A. Winters, "*Biomechanics and Motor Control of Human Movement*," John Wiley & Sons, Inc., New York. (1990)

15.   A. Goswami, "Postural stability of biped robots and the foot rotation indicator (FRI) point", in *International Journal of Robotics Research*, July 1999.

16.   A. Hofmann, M. Popovic, S. Massaquoi and H. Herr, "A Sliding Controller for Bipedal Balancing Using Integrated Movement of Contact and Non-Contact Limbs," in *International Conference on Intelligent Robots and Systems (IROS)*, (2004).